ISSN 1330-3651 (Print), ISSN 1848-6339 (Online)
Received: 22 June 2025; Accepted: 3 March 2026

https://doi.org/10.17559/TV-20250622002768
Preliminary communication

Materials Analysis of Parts of a Subsystem for the Tailings' Spreader Movement

Dušan ARSIĆ*, Ružica NIKOLIĆ, Aleksandra ARSIĆ, Malgorzata ULEWICZ, Nenad GUBELJAK, Dragan CVETKOVIĆ

Abstract: The spreaders and wheel excavators represent the key elements in the system for the tailings digging and disposal. Here are considered the parts of the caterpillar chain of the subsystem for the spreader's movement. Those parts are wheels, which were made of the cast steel 42CrMo4+QT, and the shoe links that were made of the cast steel G32NiCrMo8-5-4+QT1. Evaluation of the materials' properties of those parts included an analysis of the current state of mechanical properties as compared to corresponding properties prescribed by standards. Experimental investigations of materials included determination of their chemical compositions, tensile properties, impact toughness and macro- and micro-hardness' measurements, while the metallographic investigations were conducted, as well. Results of executed experimental investigations of the delivered wheels' and shoe links' materials have shown that their damage resistance is at the satisfactory level, i.e., that they would be damaged only in the extreme operating conditions for which they were not designed. It should be emphasized that the lateral movement of the subsystem for the spreader's motion, which can create additional loading on investigated parts, was not taken into account.

Keywords: caterpillar chain; hardness; impact strength; microstructure; operating conditions; shoe links; tailing spreader; tensile strength; wheels

1 INTRODUCTION

In open-pit mining, the problem of disposal of tailings is important from several aspects. It has to be executed efficiently and without down-times, so that the excavation process would not be interrupted. Another aspect is the design of the tailings' storage areas/facilities. They have to be close enough to the mine for efficient disposal, yet not too close to prevent eventual extension of the mining area. Lately, increasing attention is being paid to the environmental protection aspect of the tailings' disposal, i.e., how to efficiently dispose the tailings without endangering the environment. Another aspect is how to rehabilitate tailings landfills, that is, how to green those again.

Machines for tailings digging and disposal are the key elements in the system rotary Excavator, Conveyor (Transporter), Spreader (dumper) - ECS. They are "responsible" for complying with the efficiency aspect of tailings disposal; they have to be operational during the required periods, namely their damaging and/or down-times ought to be eliminated or, at least, minimized.

In certain cases, and under the extreme operating conditions, the operation of the spreader can lead to failure of the subsystems for movement of the spreader, as well as the structures connected to them. Those failures can be caused by errors in design, manufacturing errors or errors that occur during operation. Regardless of the cause, failures of high-performance machines such as spreaders always lead to large financial losses.

Literature Review

Various machines for tailings' digging and disposal were studied in articles devoted to different aspects of their manufacturing, application and operational behavior etc. The structural integrity assessment of these machines was considered in [1-3]; their design and construction in [4-6]; mechanical and structural properties of materials for their manufacturing in [7, 8]; premature damages, fractures and failures of their various parts in [9-12]; their reparation and return to operation in [13-14]; their economic efficiency in [15]; influence on environment in [16]. Since the causes of failures are often linked to fracture toughness and hardness of components, several papers from that area were analyzed, as well, [17-22]. Here is presented a brief review of some of the most interesting and important findings on those problems.

Arsić et al. [1] have analyzed the causes of damages of the boom's welded lattice structures and their behavior after the repair. Several experimental tests and calculations of stresses by the finite element method (FEM), led to the conclusion that the detected damage in the parent metal and welded joints occurred as a result of manufacturing defects. The integrity assessment of the pipe-line section from a hydropower plant was conducted in [3] by application of the failure assessment diagrams (FAD). In [4] authors presented the numerical simulation of the behavior of a supporting base structure, used for the power equipment in mining, and proposed a new design solution for it. They concluded that the part would fail due to stresses exceeding its load-carrying capacity and not due to eventual crack propagation. Vicen et al. [6] have experimentally analyzed influence of the shot peening on the wear behavior of the medium carbon C55 steel. This surface treatment resulted in compressive residual stresses, increased surface roughness and the coefficient of friction, as compared to the ground-only surfaces. Authors of [7] presented the experimental-numerical analysis of influence of temperature on mechanical properties of structural high-strength steel class S690QL. Both the experimental and numerical results have shown that the critical temperature, at which the decrease of material's mechanical properties occurs, is 550 °C. The study of authors [9] investigated the causes of premature damage to the track wheels of an ARS 2000 spreader by analyzing material properties and performing stress analyses using Hertz's theory and the finite element method (FEM). The authors concluded that design and manufacturing defects were the primary causes of the track wheels' failures. Authors of [10] presented a theoretical-experimental analysis of possible causes for fracture of a responsible machine part, which is during exploitation exposed to short, but high dynamic loading and pressure. The results pointed that the main cause was the presence of numerous unacceptable segregations of non-metallic inclusions in the used steel. An algorithm for decision flow between different methodologies for defining the quality of the base metal, due for the repair

welding, is given in [13]. It is designed to help engineers to establish and create an appropriate repair welding/hard-facing procedure to restore the integrity of a machine/structure. The problem of mining machinery efficiency is considered in [15, 16] through the impact of different types of downtimes. A multi-criterion analysis for each of the observed causes of downtimes can clearly determine the critical pattern of the downtime influence on the machine efficiency. Besides all these, it should be emphasized that all the equipment must be handled with paying attention to safety measures [17].

2 DESCRIPTIONS OF THE SPREADER AND THE CONSIDERED PARTS OF ITS MOVEMENT SUBSYSTEM

As authors of [8, 9] stated, the technical diagnostics of complex machines like the bucket wheel excavators (BWE) and its parts, should be based on predefined test procedures, history of its use under service conditions, as well as on the analysis of results carried out by the team of experts with adequate experience and knowledge in areas of design, construction, service, maintenance, reliability, etc.

The spreaders and rotary excavators are the key links in the tailings mining system. The ARs 2000 spreader, marked PA 200-2000/15+60+60, is the last link in the 6th ECS system (excavator, conveyors, spreader) for the continuous removal of tailings at the surface mine "Drmno" (Kostolac - Serbia), Fig. 1. The spreader is a product of the company SANDVIK (FLSmidth GmbH), Austria.

Figure 1 The tailings spreader PA 200-2000/15+60+60

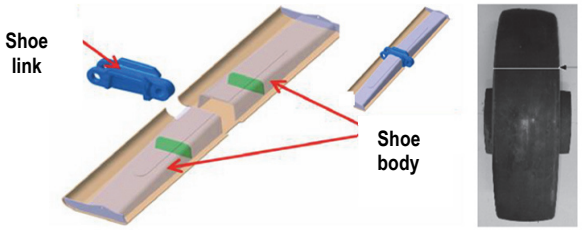

Figure 2 Basic substructures for movement of the spreader: transport shoe and wheel

The spreader superstructure rests on caterpillar chains for movement (transport) of the same length, width and height. Transporter's wheels are connected by means of cylindrical links, thus forming a transport construction with 2, 4 and 6 wheels (bogies with 2, 4 and 6 wheels), which move on caterpillar chains [9]. Basically, part of the construction of the caterpillar chain consists of wheels and shoes (links and ribs are welded to the body of the shoe), Fig. 2. The shoes are joined using cylindrical links, thus forming the shape of a caterpillar, Fig. 3. The force necessary for the movement of the spreader is transmitted from the transport reducer to the drive wheel and shoe chain. Therefore, the wheels and shoes realize the key functions of the transport reducer: the transmission of driving forces and all the loads to the ground.

Figure 3 Drive wheel and caterpillar shoe chain connected by cylindrical links

The load acting on one wheel in exploitation is F_{pt} = 500 kN. According to [9] for the wheels and shoes links of the caterpillar chain of the subsystem for movement of the spreader, the permissible compressive contact stresses under the static and dynamic loading are $\sigma_{pt,st}$ = 2000 MPa and $\sigma_{pt,dyn}$ = 1078 MPa, respectively.

Due to the fact that these parts operate in very complex conditions, it is of a great importance to make an appropriate selection of materials, as well as to carry out a strict implementation of the technology of manufacturing the wheels and shoe links, [9, 12]. In this case, according to the project documentation, the delivered wheels were made of the cast steel marked 42CrMo4 +QT, and the shoe links were made of the cast steel marked G32NiCrMo8-5-4+QT1 (in accordance with the relevant standards [18, 19]).

The objective of the research presented in this paper was evaluation of materials of the wheels and caterpillar chains' shoe links of the described tailing's spreader. That evaluation was based on comparison of the experimental results of materials' properties of the delivered parts to the standard prescribed ones.

3 EXPERIMENTAL INVESTIGATION OF PROPERTIES OF PARTS' MATERIALS

To determine whether there were deviations of the materials' mechanical properties, as compared to properties given in [20], and prescribed by the corresponding standards, experimental tests of the wheels and the shoe links materials were conducted. Those tests included determination of the materials' chemical composition, tensile properties, impact strength, and macro- and micro-hardness measurements, as well as the metallographic analysis to reveal the materials' microstructures.

3.1 Analysis of the Wheel Material Properties

The studied wheels had dimensions Ø560 × 230 mm, made of the forged pieces of the 42CrMo4 + QT steel. The part of one wheel was delivered for all the tests.

Before cutting the samples from the delivered part of the wheel, the sampling directions were agreed upon, Fig. 4, namely:

- Direction 1: Longitudinally, in the direction of the wheel axis - mark (1);
- Direction 2: Transversely, in the direction of the wheel radius, along to the material depth - mark (2).

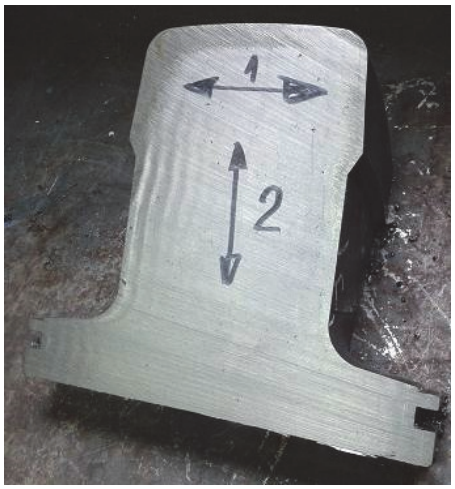

Figure 4 Appearance of the delivered part of the wheel with marked sampling directions

3.1.1 Analysis of the Wheel Material Chemical Composition

The chemical analysis of the wheel material was carried out using the ARL 360 quantometer, optical emission spectrometry, results of which are shown in Tab. 1.

Table 1 Chemical composition of the wheel material - steel 42CrMo4+QT forgings, mass %

Element	Test	Standard
C	0.40	0.38-0.45
Si	0.178	≤ 0.40
S	0.021	≤ 0.35
P	0.014	≤ 0,035
Mn	0.678	0.6-0.9
Ni	0.10	/
Cr	1.998	0.9-1.2
Mo	0.128	0.15-0.30
Pb	0.003	≤ 0.025
Cu	0.173	/

From the comparative analysis of the data presented in Tab. 1 it can be concluded that the chemical composition of the wheel material mostly corresponds to the requirements of the standard [18].

3.1.2 Tensile Test of the Wheel Material

Samples for the tensile tests were made from the submitted part of the wheel, according to the requirements of the standard EN ISO 6892-1 [21]. The tensile test was performed on a universal tension, compression and bending test machine "A. J. Amsler" (Switzerland), with a maximum measuring range of up to 98.1 (kN) on specimens shown in Fig. 5.

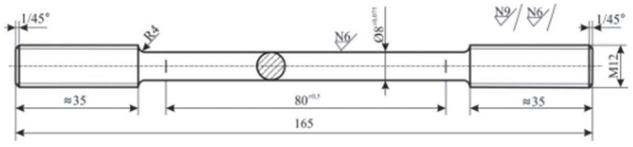

Figure 5 Drawing of the specimen for tensile testing

The test results are given in Tab. 2. They show that the mechanical characteristics of the wheel material are within the limits given in the corresponding standards [18, 19]. Standard values are given for the material thickness ≤ 160 mm.

Table 2 Mechanical properties of the wheel material at room temperature

Sample	The spreader's wheel				Steel 42CrMo4 + QT forging	
Sampling direction	1		2		1	2
Yield stress $R_{p0.2}$ / MPa	565	557	517	513	min 500	
Tensile strength Rm / MPa	768	761	740	726	min 750	
Elongation $A_{5.65}$ / %	20.5	19	16	14.5	min 10-14	
Contraction Z / %	54..4	54.4	33	30.9	min 40	

3.1.3 Impact Energy Test of the Wheel Material

Standard test samples for the impact energy testing were 10 (mm) thick, and made from the delivered part of the wheel, according to the standard requirements of EN ISO 148-1 standard (Fig. 6) [22]. The test was performed with a Charpy pendulum "A. J. Amsler", Switzerland, with a load range of 0-300 (J), at temperature –20 °C. Three samples were prepared for each testing direction and the average value was calculated. The results of the impact energy test are given in Tab. 3. Standard values are given for the material thickness ≤ 160 (mm).

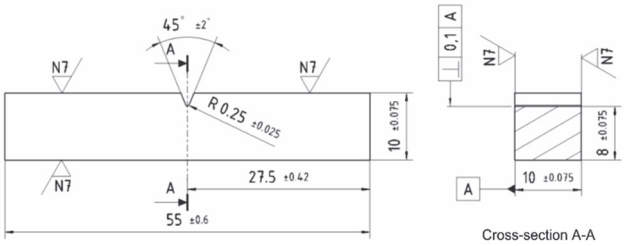

Figure 6 Drawing of the specimen for impact testing

Table 3 Results of the impact energy test of the wheel material

Sample	The spreader's wheel						Steel 42CrMo4 + QT forging	
Sampling direction	1			2			1	2
Sample #	1	2	3	1	2	3		
Impact energy KV_{300} / J	17.7	15.7	20.6	10.8	8.8	13.7	min 30	min 16
Average value / J	18			11.1			/	/

3.1.4 Hardness Test Along the Depth of the Wheel Material

After the preparation, the hardness test was carried out on the delivered part of the wheel, in the depth of the material up to 30 mm in the directions perpendicular to the thread surface of the wheel, at the points of contact with the shoe link, Fig. 7a. Tests were performed using the Rockwell method (HRC) in the directions shown in Figs. 7a and 7b, according to the requirements of the standard EN ISO 6508-1 [23]. The test results, related to the minimum and maximum hardness reference values, are given in Tab. 4 and Fig. 8. The measurement zones were chosen to examine the entire shoe link zone, which can be considered the most exposed to loads in operation.

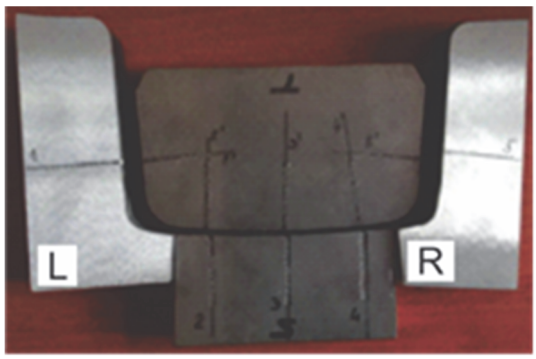

a)

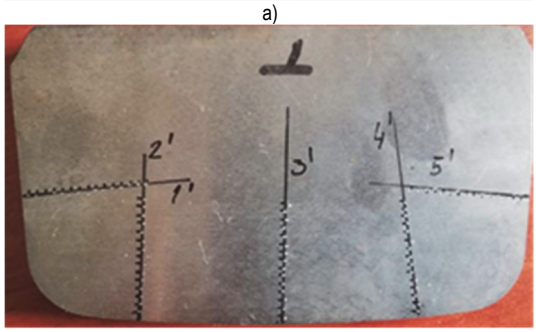

b)

Figure 7 a) Directions of the hardness measurements in the contact zone of the wheel and the shoe link; b) Details of the hardness measurements positions (lines 1 to 5, Tab. 4)

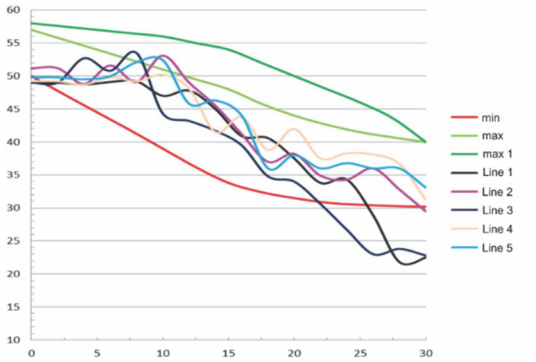

Figure 8 Hardness variation along the material's depth with minimum and maximum values

Table 4 Results of the hardness measurements along the material depth of the wheel

Points / Lines	*d* / mm*	1'	2'	3'	4'	5'
1	2	51.2	49	49.2	49.8	51.2
2	4	48.8	52.7	48.7	49.5	48.8
3	6	51.6	50.8	49.8	50	51.6
4	8	49.1	53.5	49.2	52.1	49.1
5	10	53.1	44.3	50.2	52.4	53.1
6	12	49	43.2	48.1	45.8	49
7	14	45.5	41.7	41.5	46.3	45.5
8	16	41.2	39.5	43.8	44	41.2
9	18	37	34.8	38.8	36	37
10	20	38.2	34	42	38	38.2
11	22	34.9	30.6	37.5	36	34.9
12	24	34.3	26.7	38.3	36.8	34.3
13	26	36	23	38.1	36	36
14	28	32.8	23.8	36.7	36	32.8
15	30	29.5	22.8	31.3	33.1	29.5

**d* - distance between the measuring points

By analyzing the results, it can be concluded that the wheel material is homogeneous since there are no major deviations in the results in different measurement zones.

The obtained hardness results can be converted into tensile strength and yield stress using the expressions [24]:

$$\sigma_{\mathrm{UTS,HV}} = -99.8 + 3.734Hv\,,$$

$$\sigma_{\mathrm{YS,HV}} = -90.7 + 2.876Hv\,.$$

By calculating the strength according to the mentioned formulas, a slightly higher strength is obtained than that prescribed for the tested steel. High strength in the surface zones of the track material (acted by the wheel) can lead to peeling of the material and significant damage to the track [9].

3.1.5 Investigation of the Wheel Material's Microstructure

The metallographic analysis of the microstructure was performed on a "METAVAL" metallographic microscope ("Carl Zeiss", Jena, Germany), using the bright-field technique. The test part and locations of the samples, taken for metallographic tests, are shown in Fig. 9. Samples etching was done by the 3% nitric acid alcoholic solution. The results of the test with a magnification of 100× are given in Fig. 9.

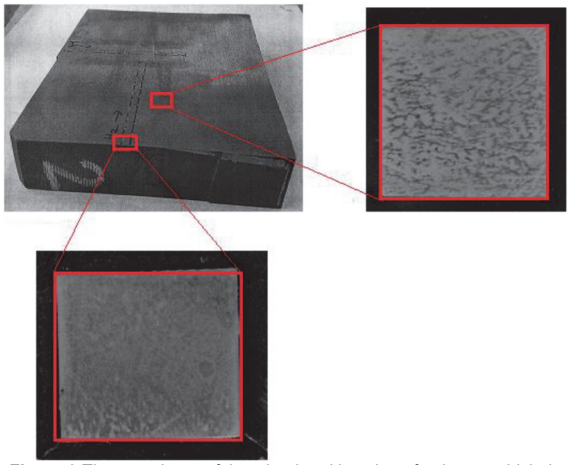

Figure 9 The tested part of the wheel and location of points at which the samples were taken

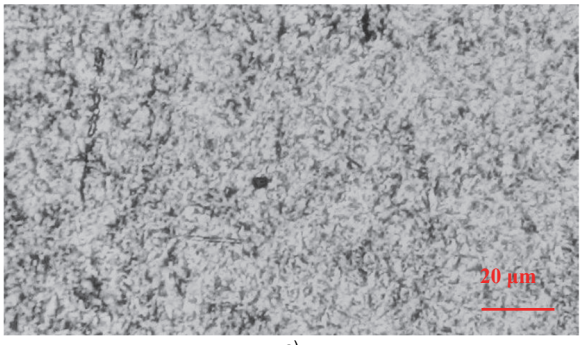

a)

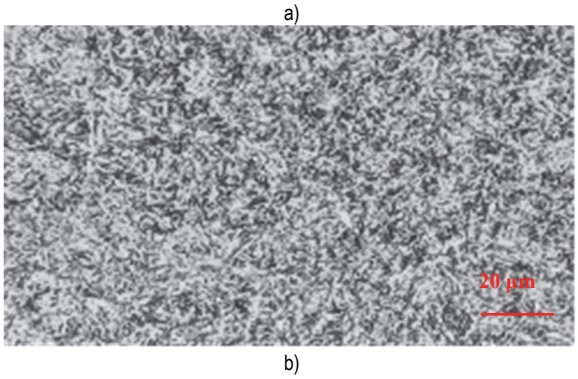

b)

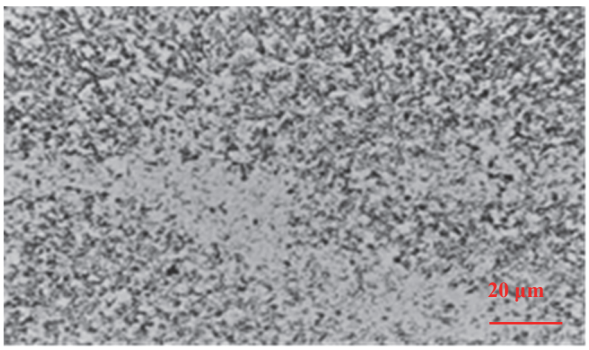

c)

Figure 10 Results of microstructure investigations: a) Surface zone; b) Subsurface zone; c) Specimen bulk

The microstructure in the surface and subsurface zone of the examined piece (at depth of 3 mm from the sample surface) consists of martensite (Fig. 10a and 10b), and the microstructure in the bulk (at depth of 10 mm from the sample surface) of martensite and bainite, Fig. 10c, which corresponds to the material class of steel forging 42CrMo4 +QT.

4 ANALYSIS OF THE SHOE LINK MATERIAL PROPERTIES

According to the data of the manufacturer's documentation, the shoe links of the caterpillar chains for the movement of the spreader, were of dimensions 880 × 422 mm [20]. The material of the link in question is a steel casting marked G32NiCrMo8-5-4+QT1, according to the EN 10293 standard [19].

To check the conformity of the material characteristics with the standard ones a part of the shoe link was submitted for testing.

Before cutting the samples from the delivered part of the shoe link, the sampling directions were agreed upon, Fig. 11, namely:

Direction 1: Parallel to the thread surface of the shoe - mark (1);

Direction 2: Perpendicular to the thread surface, along the material depth - mark (2).

The appearance of the delivered part of the shoe link with marked sampling directions is shown in Fig. 11.

Figure 11 Appearance of the delivered part of the shoe link with marked sampling directions

4.1 Analysis of the Shoe Link Material Chemical Composition

Chemical composition analysis of the shoe link material was carried out using the ARL 360 quantometer by optical emission spectrometry, results of which are shown in Tab. 5. From comparison of the obtained results to values prescribed by the standard, one can see that the chemical composition of the shoe link material generally corresponds to the requirements given in the standard [23], except for the percentage of carbon (C) which is significantly lower than prescribed.

Table 5 Chemical composition of the shoe link material - steel G32NiCrMo8-5-4+QT1 forgings, mass %

Element	Test	Standard
C	0.160	0.28-0.35
Si	0.395	≤ 0.60
S	0.003	≤ 0.015
P	0.009	≤ 0,002
Mn	0.694	0.60 - 1.00
Ni	1.625	1.60 - 2.10
Cr	1.142	1.0 - 1.6
Mo	0.380	0.30 - 0.50
Pb	0.039	/
Cu	0.160	0.28 - 0.35

4.2 Tensile Test of the Shoe Link Material

Test samples were made from the submitted part of the shoe link, according to the requirements of the standard EN 10293 [19]. The test was performed on a universal tensile, compression and bending test machine "A. J. Amsler" Switzerland, with the maximum measuring range up to 98.1 kN. The results of test performed at the room temperature, given in Tab. 6, were within the limits given in the standards [18, 19].

Table 6 Mechanical properties of the shoe link material at room temperature

Sample	The spreader's wheel				Steel G32NiCrMo8-5-4+QT1, forging	
Sampling direction	1		2		1	2
Yield stress $R_{p0.2}$ / MPa	637	647	647	656	min 650	
Tensile strength Rm / MPa	792	804	802	822	820-1200	
Elongation $A_{5.65}$ / %	17.75	17	15	15.5	min 10-16	
Contraction Z / %	54.4	53.6	51	48.3	/	

The obtained results have shown slightly lower values of the yield stress and tensile strength in 3 out of 4 tested samples, but those deviations are minimal and it was estimated that these results can be considered as valid.

4.3 Impact Energy Test of the Shoe Link Material

Standard test samples for the impact energy testing, 10 (mm) thick, were made from the delivered part of the shoe link, according to the requirements of EN ISO 148-1 standard [22]. The test was performed with a Charpy pendulum "A. J. Amsler", Switzerland, with a range of 0-300 J, at temperature –20 °C. Three samples were prepared for each testing direction and the average value was calculated. The results of the impact energy test, given in Tab. 7, show that they are within the limits given in the standard.

Table 7 Results of the impact energy test of the shoe link material

Sample	The spreader's wheel						Steel G32NiCrMo8 -5-4+ QT1, forging	
Sampling direction	1			2			1	2
Sample #	1	2	3	1	2	3		
Impact energy KV_{300} / J	52	42.2	44.1	27.5	26.5	29.4	min 30	min 16
Average value / J	46.1			27.8			/	/

4.4 Hardness Test Along the Depth of the Shoe Link Material

After the samples' preparation, the hardness test was carried out on the delivered part of the shoe link, at different distances from the sample's surface, d, in the depth of the material up to 30 mm, in the directions perpendicular to the thread surface of the shoe link, at the points of contact with the wheel, Fig. 12. Tests were performed using the Rockwell method, according to the requirements of the standard EN ISO 6508-1 [23]. The test results, related to the minimum and maximum hardness reference values, are given in Tab. 8 and Fig. 11.

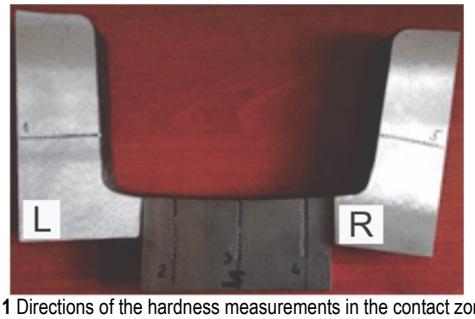

Figure 11 Directions of the hardness measurements in the contact zone of the shoe link and the wheel

Table 8 Results of the hardness measurements along the material depth of the shoe link

Points / Lines	*D* / mm	1'	2'	3'	4'	5'
1	2	42	37.2	40	40	41.2
2	4	42.8	45.3	45.2	45.7	47.2
3	6	43.8	47.2	45.8	47.2	47.8
4	8	42.5	45.4	45.8	46.3	46.2
5	10	41.8	40.2	41.4	45.3	39.8
6	12	41.8	33	39.2	40.2	32
7	14	38.8	36.8	24.2	23.5	19.2
8	16	21.5	22.1	25.5	23.4	21.5
9	18	23.2	23.6	26	24.2	22.3
10	20	24.5	23.2	25.5	24	21.8
11	22	25.5	20.4	26.1	17.3	21.6
12	24	22	18.3	20	18.2	24
13	26	25.2	18.3	19	20.5	24.3
14	28	22.2	19.3	21.2	18.3	20
15	30	27.3	21.8	21.5	19.8	22.4

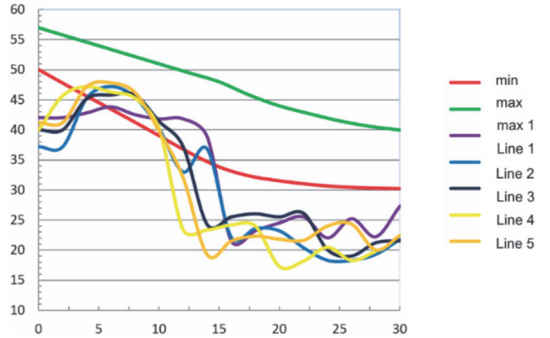

Figure 12 Hardness variation along the material's depth with minimum and maximum values

4.5 Investigation of the Shoe Link Material's Microstructure

The metallographic analysis of the microstructure was performed on a "METAVAL" metallographic microscope "Carl Zeiss", Germany, using the bright-field technique. The test part and the locations of the samples, taken for metallographic tests, are shown in Fig. 13. Samples etching was done by the 3% nitric acid alcoholic solution.

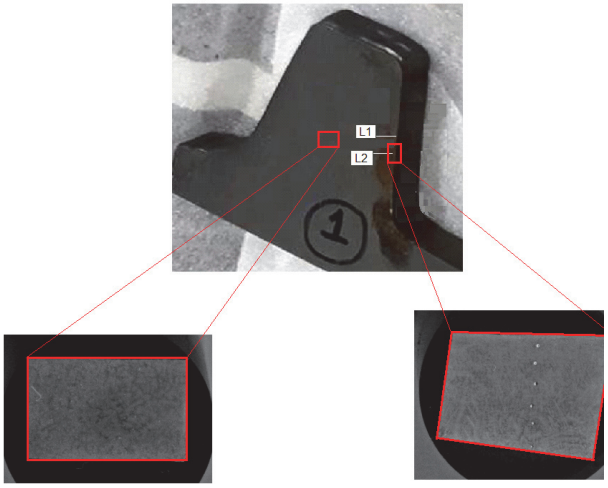

Figure 13 The tested part of the shoe link and location of points at which the samples were taken

The results of the test with a magnification of 100× are given in Fig, 14. The microstructure in the surface and subsurface zone of the tested piece, at a depth of 3 (mm) from the surface, consists of martensite (Figs. 14a and 14b), and the microstructure in the bulk of the test piece sample, at a depth of 10 mm from the surface, consists of bainite and martensite, Fig. 14c.

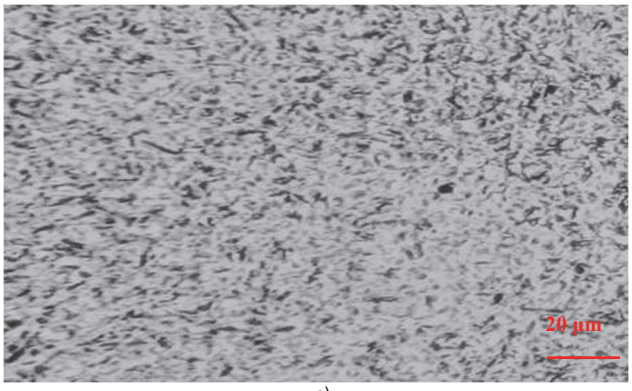

a)

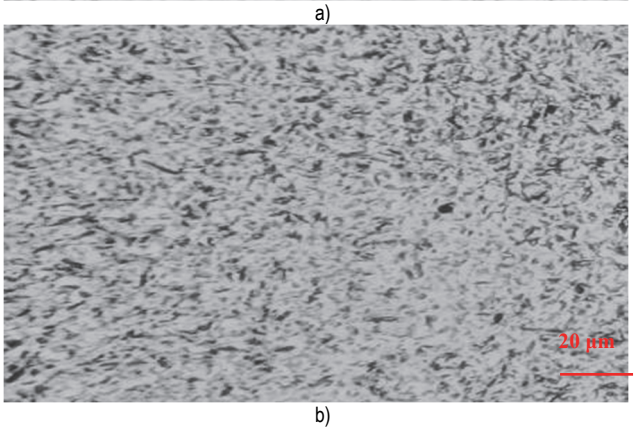

b)

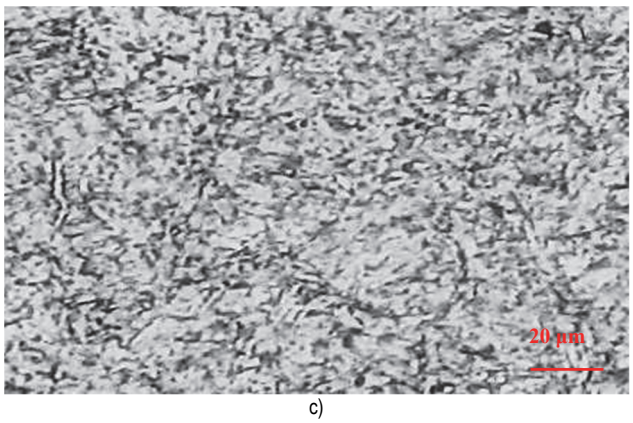

c)

Figure 14 Results of microstructure investigations: a) Surface zone; b) Subsurface zone; c) Specimen bulk

5 DISCUSSION AND CONCLUSIONS

The objective of this research was analysis of certain parts materials' compliance with requirements of the corresponding standards. Those parts were designed to sustain certain loads, under certain loading and operating conditions, and due to that were made of the selected materials, i.e., those materials fulfilled the requirements concerning the mechanical properties, hardness and microstructure, which would guarantee that the parts would perform the designed tasks. The parts in question were the wheel (made of cast steel 42CrMo4+QT) and shoe link (made of cast steel G32NiCrMo8-5+QT) of the subsystem for movement of the tailings' spreader operating at a surface mine in Serbia. To realize this research objective, experimental tests were performed on samples of those materials, which were cut from the corresponding two parts that were taken from the actual caterpillar chain structure.

For the wheel material (cast steel 42CrMo4+QT) the chemical composition was completely within the limits prescribed by the corresponding standard, while for the shoe link material (cast steel G32NiCrMo8-5+QT) the content of carbon was much lower than the value prescribed by standard. Lower carbon content can lead to poorer mechanical properties of the material, lower hardness and hardenability.

What concerns the mechanical properties, for the wheel material all the values were satisfying the standard prescribed ranges, while, for the shoe link material the yield stress and tensile strength values for 3 samples were slightly below the standard ones. The measured values were 637 to 645 MPa vs. the standard value of 650 MPa for the former and from 792 MPa to 802 MPa vs. the minimum standard value of 820 MPa for the latter. However, the deviations from the standard values were really small, less than 2% and 3.4%, respectively, for the two materials; thus, the measured values could be considered as valid.

The measured impact energy values, for the wheel material, for both selected measurements directions were not in accordance with the corresponding standard. For the direction 1 (direction of the wheel axis) the average measured value was 18 J vs. min 30 J - standard value, and for the direction 2 (direction of the wheel radius) the average measured value was 11.1 J vs 16 J - standard value. These results, i.e., the significantly lower values than the standard prescribed ones, may indicate a poor quality of the wheel material, especially in terms of impact resistance and the possibility for the cracks appearance in exploitation. Similar researches showed that could be potential problem [25-27]. For the shoe link material, for the direction 1 (parallel to the thread surface of the shoe) the average measured value was 46.1 J vs. min 30 J - standard value, and for the direction 2 (perpendicular to the thread surface, along the material depth), the average measured value was 27.8 J vs. min 16 J - standard value.

The measured hardness values, on the surface, and the distribution along the depth of the specimen up to 30 (mm), were within the range between the minimum and maximum permissible values.

The microstructures of both materials were similarly "distributed". At the samples' surfaces and the subsurface zones, the structures consisted of martensite, while within the materials' bulk (at depth of 10 mm below the surface) the structures consisted of martensite and bainite. Those structures are adequate for the type of parts' materials that were considered.

Based on the results of the experimental tests performed on one delivered wheel and one delivered shoe link, it can be concluded that those materials are adequate for the designed purposes of those parts, and the designed operating conditions. The damage and fracture of the wheels and shoe links of the caterpillar chain of the subsystem for the movement of the spreader PA 200-2000/15+60+60, could occur only under the extreme operating conditions, for which they were not designed.

Acknowledgements

This research was partially financially supported by the project No. 09I03-03-V03-00036, funded by the EU NextGenerationEU through the Recovery and Resilience Plan for Slovakia and by the Ministry of Education, Science and Technological Development of the Republic of Serbia through grants: TR35024.

6 REFERENCES

[1] Arsić, M., Flajs, Ž., Sedmak, A., Veg, E., & Sedmak, S. (2021). Structural integrity assessment of welded bucket-wheel boom. *Structural Integrity and Life*, *21*(2), 201-206. https://doi.org/10.4028/p-15iqnw

[2] Vulovic, S., Zivkovic, M., Pavlovic, A., Vujanac, R., & Topalovic M. (2023). Strength Analysis of Eight-Wheel Bogie of Bucket Wheel Excavator. *Metals*, *13*(3), 466. https://doi.org/10.3390/met13030466

[3] Gasper, F., Gubeljak, N., & Chapetti, M. D. (2023). Fatigue integrity analysis of a howitzer cannon by using a fracture mechanics approach. *Engineering Fracture Mechanics*, *292*, 109653. https://doi.org/10.1016/j.engfracmech.2023.109653

[4] Gasper, F., Nenad, G., & Chapetti, M. D. (2023). Fatigue life of a howitzer cannon. *Procedia Structural Integrity*, *48*, 398-405. https://doi.org/10.1016/j.prostr.2023.08.034

[5] Vicen, M., Bokůvka, O., Trško, L., Drbul, M., Nikolić, R., & Nový F. (2022). Influence of shot peening on the wear behaviour of medium carbon steel. *Production Engineering Archives*, *28*(3), 241-245. https://doi.org/10.30657/pea.2022.28.29

[6] Arsić, D., Djordjević, M., Živković, J., Sedmak, A., Aleksandrović, S., Lazić, V., & Rakić, D. (2016). Experimental-numerical study of tensile strength of the high-

strength steel S690QL at elevated temperatures. *Strength of Materials*, *48*(5), 687-695. https://doi.org/10.1007/s11223-016-9812-x
[7] Arsić, M., Arsić, D., Flajs, Ž., Grbović, A., & Todić A. (2021). Application of non-destructive testing for condition analysis, repair of damages and integrity assessment of vital steel structures. *Russian Journal of Nondestructive Testing*, *57*(10), 918-931. https://doi.org/10.1134/S1061830921100053
[8] Arsić, M., Bošnjak, S., Odanović, Z., Dunjić, M., & Simonović, A. (2012). Analysis of the spreader track wheels premature damages. *Engineering Failure Analysis*, *20*, 118-136. https://doi.org/10.1016/j.engfailanal.2011.11.005
[9] Lazić, V., Čukić, R., Aleksandrović, S., Milosavljević, D., Arsić, D., Nedeljković, B., & Đorđević, M. (2014). Techno-economic justification of reparatory hard facing of various working parts of mechanical systems. *Tribology in Industry*, *36*(3), 287-292.
[10] Arsić, D., Nikolić, R., Lazić, V, Arsić, A., Savić, Z., Djačić, S., & Hadzima, B. (2019). Analysis of the cause of the girth gear tooth fracture occurrence at the bucket wheel excavator. *Transportation Research Procedia*, *40,* 413-418. https://doi.org/10.1016/j.trpro.2019.07.060
[11] Petrović, A., Momčilović, N., Sedmak, A., Đorđević, B, Dorin R., Milošević-Mitić, V., & Bogojević, A. (2025). Reliability-based approach for structural integrity assessment of a bucket wheel excavator. *Theoretical and Applied Fracture Mechanics*, *136*, 104849. https://doi.org/10.1016/j.tafmec.2025.104849
[12] Arsić, M., Bošnjak, S., Odanović, Z., Dunjić, M., & Simonović, A. (2012). Analysis of the spreader track wheels premature damages. *Engineering Failure Analysis*, *20*, 118-136. https://doi.org/10.1016/j.engfailanal.2011.11.005
[13] Crupi, V., Guglielmino, E., Maestro, M., & Marinò, A. (2009). Fatigue analysis of butt welded AH36 steel joints: Thermographic Method and design S-N curve. *Marine Structures*, *22*(3), 373-386. https://doi.org/10.1016/j.marstruc.2009.03.001
[14] Jovicic, G., Nikolic, R., Zivkovic, M., Milovanovic, D., Jovicic, N., Maksimovic, S., & Djordjevic, J. (2013). An estimation of the high-pressure pipe residual life. *Archives of Civil and Mechanical Engineering*, *13*(1), 36-44. https://doi.org/10.1016/j.acme.2012.11.002
[15] Małysa, T. (2025) Application of selected Lean tools in the improvement of work safety in the use of machinery. *Production Engineering Archives*, *31*(1), 129-136. https://doi.org/10.30657/pea.2025.31.12
[16] EN 10250-3: Open die steel forgings for general engineering purposes - Part 3: Alloy special steels, European Committee for Standardization, 2012.
[17] EN 10293: Steel castings - Steel castings for general engineering uses, European Committee for Standardization, 2015.
[18] Spreader PA 200-2000/15+60+60, manufacturer documentation, 2017. https://doi.org/10.2307/j.ctv11smfg2.5
[19] EN ISO 6892-1: Metallic materials - Tensile testing - Part 1: Method of test at room temperature, European Committee for Standardization, 2016.
[20] EN ISO 148-1: Metallic materials - Charpy pendulum impact test - Part 1: Test method, European Committee for Standardization, 2016.
[21] EN ISO 6508-1: Metallic materials - Rockwell hardness test - Part 1: Test method, European Committee for Standardization, 2015.
[22] Pavlina, E. J. & Van Tyne C. J. (2008). Correlation of yield strength and tensile strength with hardness for steels. *Journal of Materials Engineering and Performance*, *17*(6), 888-893. https://doi.org/10.1007/s11665-008-9225-5
[23] Świt, G., Dzioba, I., Ulewicz, M., Lipiec, S., Adamczak-Bugno, A., & Krampikowska, A. (2023). Experimental-numerical analysis of the fracture process in smooth and notched V specimens. *Production Engineering Archives*, *29*(4), 444-451. https://doi.org/10.30657/pea.2023.29.49
[24] Bjelajac, E., Skumavc, A., Lojen, G., Manjgo, M., & Vuherer, T. (2024). Comparison of the mechanical properties of hard facings made by standard coated stick electrodes and a newly developed rectangular stick electrode. *Materials, 17*(9), 2051. https://doi.org/10.3390/ma17092051
[25] Perković, S., Radaković, Z., Burzić, Z., Sedmak, S., Sedmak, A., & Radović, Lj. (2023). Stress concentration effects on toughness value of duplex steel S32750. *Structural Integrity and Life*, *23*(1), 3-7.
[26] Stodola, J. & Stodola, P. (2024). Accelerated reliability tests of characteristics of off-road vehicles and their parts. *Transactions of FAMENA*, *48*(2), 31-44. https://doi.org/10.21278/TOF.482049422

Contact information:

Dušan ARSIĆ, Associate Professor
(Corresponding author)
Faculty of Engineering,
University of Kragujevac,
Sestre Janjić 6, 34000 Kragujevac, Serbia
E-mail: dusan.arsic@fink.rs

Ružica NIKOLIĆ, Researcher
Research Centre,
University of Žilina,
Univerzitna 8215/1, 01008 Žilina, Slovakia
E-mail: ruzica.nikolic@uniza.sk

Aleksandra ARSIĆ, Teaching Assistant
Faculty of Mechanical Engineering,
University of Belgrade,
Kraljice Marije 16, 11120 Belgrade, Serbia
E-mail: aarsic@mas.bg.ac.rs

Malgorzata ULEWICZ, Professor
Faculty of Civil Engineering,
Czestochowa University of Technology,
ul. Akademicka 3, 42-201 Częstochowa, Poland
E-mail: malgorzata.ulewicz@pcz.pl

Nenad GUBELJAK, Professor
Faculty of Mechanical Engineering,
University of Maribor,
Smetanova ul. 17, 2000 Maribor, Slovenia
E-mail: nenad.gubeljak@um.si

Dragan CVETKOVIĆ, Senior Research Associate
Institute for information technologies Kragujevac,
University of Kragujevac,
Jovana Cvijića bb, 34000 Kragujevac, Serbia
E-mail: dragan_cw8202@yahoo.com